Design and optimization of the seed conveying system for belt-type high-speed corn seed guiding device

Yifei Li[1,2], Wenqi Zhou[1*], Chengcheng Ma[2], Zhaohua Feng[3], Jinwu Wang[1], Shujuan Yi[2], Song Wang[2]

(1. *College of Engineering, Northeast Agricultural University, Harbin 150030, China*;
2. *College of Engineering, Heilongjiang Bayi Agricultural University, Daqing 163000, Heilongjiang, China*;
3. *Agricultural Engineering Department, Qitaihe Vocational Technician College, Qitaihe 154600, Heilongjiang, China*)

Abstract: Seeding is an important part of improving corn yield. Currently, seed guide tubes are mostly used as transport devices. But the existing seed guide tubes cannot meet the requirements or achieve the goal of fixing the seed falling trajectory. A seed collision phenomenon occurs occasionally. So, in response to the problems that the seeds and seed guide tube collide or bounce under high speed operation, which results in a lower sowing qualification rate and poor spacing uniformity, a seed receiving and conveying system comprising a belt-type high-speed corn seed guiding device was designed and optimized, to meet the needs of high-speed precision sowing operations and improve the spacing uniformity.The factors affecting the seed conveying performance were obtained by analyzing the mechanical properties of the seeds at various movement stages. These factors were the number of seed cavities between adjacent seeds, the forward speed, the height from the ground, and the installation angle. Single factor simulation experiments were conducted by selecting the paddle spacing as the test factor and using the pass rate, reseeding rate, omission rate and coefficient of variation as the evaluation indexes to investigate the influence of the paddle spacing on the seed guide performance of the device and further determine the structural parameters of the paddle belt. Orthogonal rotation combination tests of three factors and five levels were also conducted through bench testing.Then the test outcomes were optimized. The results indicated that the best results were obtained when the number of seed cavity intervals between adjacent seeds was 5.16, the installation angle was 79.40°, and the height from the ground was 31.84 mm. At this time, the qualified rate was 98.49%, the repeated sowing rate was 0.48%, the missed sowing rate was 1.03%, and the coefficient of variation was 6.80%. Experiments were used to validate the optimization results, and all of the obtained index data satisfied the criteria for accurate and quick corn sowing. The study's findings can serve as a theoretical foundation for a belt-type high-speed corn seed guiding device optimization test.

Keywords: corn, high-speed sowing, belt-type seed guide device, test
DOI: 10.25165/j.ijabe.20241702.8427

Citation: Li Y F, Zhou W Q, Ma C C, Feng Z H, Wang J W, Yi S J, et al. Design and optimization of the seed conveying system for belt-type high-speed corn seed guiding device. Int J Agric & Biol Eng, 2024; 17(2): 123–131.

1 Introduction

Precision sowing, which is the current trend in corn sowing technology, has the advantages of saving seeds and reducing the labor-intensive task of later-stage seedling thinning, and can effectively guarantee the consistency of seed spacing and sowing quantity[1-3]. Higher requirements for seeders simultaneously arise from the need for efficient operation[4]. A high-speed seed guiding system and a precision seed metering system make up the majority of a high-speed precision seeder. When they work together, seeds can be deposited into the seed ditch quickly and precisely[5-8]. However, the main factors that influence the sowing performance are the seed bounce and collision in a high-speed seed guiding device[9]. The degree of bounce and collision also rises as the working speed increases, which has a significant impact on the seed-throwing accuracy. Therefore, it is crucial to conduct research on fast seed guiding technology.

Belt-type corn guiding is a sowing technique that makes use of a belt conveyor to move seeds from the seed disk to the seed ditch. This technique can increase the sowing accuracy and uniformity and is appropriate for high-speed precision seeders[10]. Farmers and researchers are interested in this seed-guiding technique because it can increase crop production efficiency and quality, decrease manual labor, and reduce planting costs.

The US John Deere company developed a high-speed planter with a brush belt seed delivery device that can adjust the speed of the brush belt in real time to make the horizontal component of the seed velocity into the seedbed cancel out with the planter's forward velocity, achieving zero-speed seeding and improving the seeding accuracy and uniformity[11]. Precision Planting Company developed a high-speed planter with a belt-driven seed delivery device that can transfer the seeds from the seed meter to the partitions on the belt and transport them to the furrow. The belt matches the planter's forward velocity, ensuring seed landing stability[12]. Wei et al.[13]

Received date: 2023-07-17 **Accepted date:** 2024-03-06
Biographies: Yifei Li, MS, Senior Experimentalist, research interest: agricultural mechanization engineering, Email: lyifei1990@126.com; **Chengcheng Ma**, PhD candidate, research interest: agricultural mechanization engineering, Email: 1601147341@qq.com; **Zhaohua Feng**, MS, Teaching Assistant, research interest: agricultural mechanization engineering, Email: 847115864@qq.com; **Jinwu Wang**, PhD, Professor, research interest: agricultural mechanization engineering, Email: jinwuw@neau.edu.cn; **Shujuan Yi**, PhD, Professor, research interest: agricultural mechanization engineering, Email: yishujuan_2005@126.com; **Song Wang**, PhD candidate, research interest: agricultural mechanization engineering, Email: 2941904409@qq.com.
***Corresponding author: Wenqi Zhou**, PhD, Professor, research interest: agricultural mechanization engineering. College of Engineering, Northeast Agricultural University, Harbin 150030, China. Tel: +86-155460813294, Email: zhouwenqi1989@163.com.

compared different types of belt seed delivery devices and found that the push-type device had the highest seeding accuracy and the lowest coefficient of variation of seed spacing, but the complexity and cost of it structure were also higher, while the brush belt and belt drive devices had better performance and economy, making them suitable for high-speed planter applications. Nielsen[14] conducted field trials on different types of corn planters at different operating speeds and found that planters with belt seed delivery devices had higher qualified rates and lower coefficients of variation of seed spacing at high-speed operations, while planters with air pressure seeding devices performed better at low-speed operations. Zhu et al.[15] optimized the structure and parameters of the brush belt seed delivery device, proposed a linear seeding method based on the synchronous movement of the brush belt and the seed meter, and verified its seeding performance through experiments. The results showed that this method could effectively reduce the coefficient of variation and miss rate of seed spacing. Chen et al.[16] designed and optimized the structure and parameters of a flexible belt seed delivery device, proposed a linear seeding method based on the synchronous movement of the flexible belt and the seed plate, and verified its seeding performance through experiments. The results showed that this method could effectively reduce the coefficient of variation and miss rate of seed spacing and improve the seeding accuracy and uniformity. Liu et al.[17] conducted dynamic analysis and simulation on the flexible belt seed delivery device, established a contact force model between the flexible belt and the seeds, and analyzed the effects of parameters such as tension, speed, and stiffness of the flexible belt on the seeding process, providing a theoretical basis for the design and optimization of the flexible belt seed delivery device.

In conclusion, the current belt-type corn seed guide device has a moderately good adaptability to high-speed operation, but the versatility is poor because most of them require a corresponding seed metering device to be used with them. In light of this, this paper designs and optimizes a seed conveying system based on the belt-type seed guiding device created by Precision Planting Company, which further improves the accuracy and controllability of seed movement during the seed guiding process.

2 Materials and methods

2.1 Structure and working principle of belt-type high-speed corn seed guiding device

As seen in Figure 1, the driving motor, gear box, finger wheel, seed conveying belt, and other parts make up the majority of the structure of a belt-type high-speed seed guiding device.

The seed conveying system can be broken down into three operational phases, namely receiving seed, transporting seed, and throwing seed. The finger wheels take the seeds off the seed disk and throw them into the seed cavity of the seed conveying belt in the seed receiving stage. The seeds move downward with the seed conveying belt in the seed transporting stage. When moving to the seed throwing position, the seeds are thrown into the seed ditch under the push of the pick, and this is the seed throwing stage. Throughout the entire movement process, the seeds are contained in a closed seed cavity, which guarantees the stability of seed movement.

2.2 Design of core components for seed receiving system

The feeder wheel is the core component of the seed receiving system, and its reasonable structure and parameter design will directly affect the working effect of the whole seed receiving system.

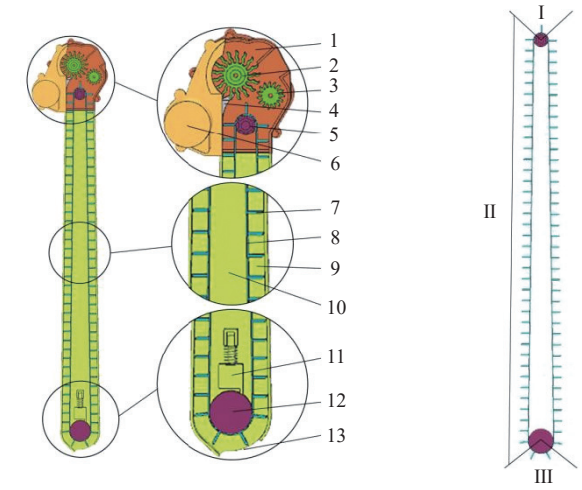

a. Belt-type high-speed corn seed guiding device b. Seed conveyor belt

1. Gear box. 2. Primary feeder wheel. 3. Auxiliary feeder wheel. 4. Seed cleaning claw. 5. Driven pulley. 6. Driving motor. 7. Pick. 8. Baseband. 9. Seed cavity. 10. Case. 11. Pre-tightening spring. 12. Driven pulley. 13. Throwing position. Ⅰ. Receiving seed. Ⅱ. Transporting seed. Ⅲ. Throwing seed.

Figure 1 Structure diagram of the belt-type high-speed corn seed guiding device

2.2.1 Gap width of seed receiving

In this study, the seed-receiving gap width is designed according to the external dimensions and adsorption posture of the corn seeds, which is mainly divided into vertical- and lateral-lying. The seed-receiving gap width should ensure that the vertical seeds can be completely clamped (Figure 2a) and that the lateral-lying seeds can pass through (Figure 2b), so elastic fingers should be installed on the wheel body and the seeds should be removed by rotating clamping. Assuming that the corn seeds are adsorbed at the center of the hole, there is:

$$t_a \le s \le t_b \tag{1}$$

where, t_a is the thickness of the vertical corn kernel tip, which is generally 1.0–1.5 mm and here t_a = 1.5 mm; t_b is the thickness of the end of the vertical corn grain, which is generally 2.5–3.0 mm and here t_b = 3.0 mm; s is the seed-receiving gap width, mm.

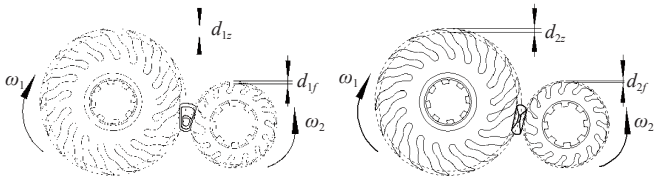

a. Vertical grain clamped state b. Lateral-lying grain clamped state

Figure 2 Schematic diagram of corn seeds in different states passing through the gap of the feeder wheel

Equation (1) shows that 1.5≤s≤3. In order to make the feeder wheel receive seeds to the maximum extent, the median value of s here is 2.3 mm.

2.2.2 Finger deformation parameters

As can be seen from Figure 2, the equations for calculating the maximum total deformation and the minimum total deformation of the fingers of the main and auxiliary feeder wheels can be expressed as follows:

$$\begin{cases} d_{\max} = d_{1z} + d_{1f} = w_b - s \\ d_{\min} = d_{2z} + d_{2f} = t_b - s \end{cases} \tag{2}$$

where, w_b is the width of the end of the corn grain lying laterally on its side, which is generally 7.0–8.5 mm and here w_b = 8.5 mm; d_{1z} is the maximum deformation of the finger of the main feeder wheel, mm; d_{2z} is the minimum deformation of the finger of the main feeder wheel, mm; d_{1f} is the maximum deformation of the finger of the auxiliary feeder wheel, mm; d_{2f} is the minimum deformation of the finger of the auxiliary feeder wheel, mm; $d_{\max}$ is the maximum total deformation of the fingers of the main and auxiliary feeder wheels, mm; $d_{\min}$ is the minimum total deformation of the fingers of the main and auxiliary feeder wheels, mm.

According to Equation (2), the minimum deformation value is 0.7 mm, and the maximum deformation value is 6.2 mm.

2.2.3 Finger structure and parameters

The finger structure diagram of the main and auxiliary feeder wheels is shown in Figure 3. The fingers adopt an inclined arc structure. For the convenience of gripping seeds, it is initially determined that the tilt angle (α) of the fingers for the main wheel is 30° and the finger spacing angle (β) is 21°, so the number of fingers of the main wheel is 17; when the tilt angle (α') of the fingers of the auxiliary wheel is 30° and the spacing angle (β') of the fingers is 24°, the number of fingers of the auxiliary wheel is 15. The finger thickness of the main feeder wheel is 2.5 mm, and that of the auxiliary feeder wheel is 2 mm. When receiving seeds, the maximum total deformation value ($d_{\max}$) of the main and auxiliary fingers is 6.2 mm. If the deformation value (ab) of the main wheel is 5 mm and the deformation value ($a'b'$) of the auxiliary wheel is 1.2 mm, the length (ac) of the main wheel is 10 mm, and the length ($a'c'$) of the auxiliary wheel is 3 mm.

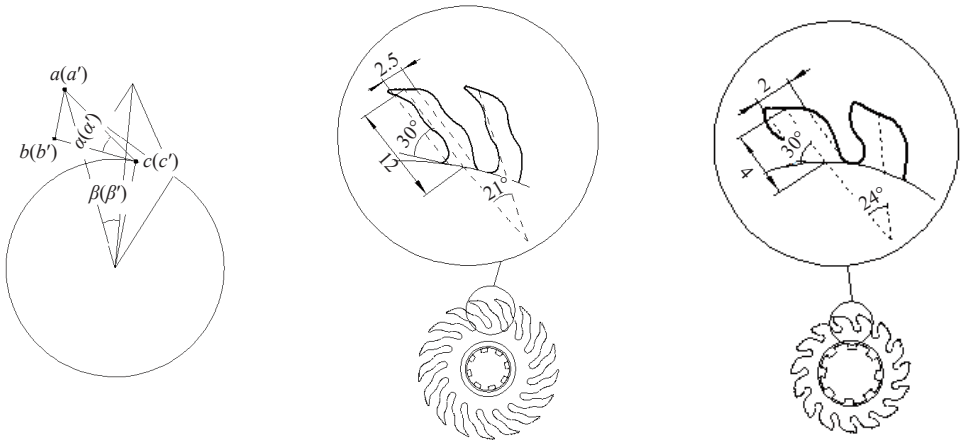

a. Finger structure diagram b. Finger of main feeder wheel c. Finger of auxiliary feeder wheel

Figure 3 Schematic diagram of finger structure of main and auxiliary feeder wheels

In order to increase the friction coefficient between the fingers and the seeds, herringbone lines can be added to the fingers, as shown in Figure 4. Herringbone lines have the characteristics of a high friction coefficient, good anti-skid performance and guidance, which can make the contact between the feeder wheel and the seed more firm and stable, thus improving the stability and accuracy of the seed entering the seed cavity.

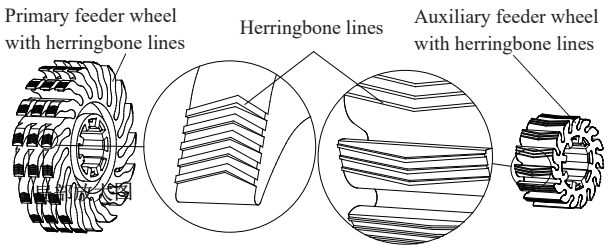

Figure 4 Main and auxiliary feeder wheel with herringbone lines added

2.2.4 Design of core components for seed conveying system

The main part of the seed conveying system is the belt for the seeds. The seed cavity, which is the center of the seed conveying belt, is made up of two picks. The seed conveying effect is directly influenced by the structural characteristics of the seed cavity.

2.2.5 Calculation of pick size parameters

The length of the cavity should be greater than the maximum size of the seeds, and the pick's length and width should be greater than or equal to the width and thickness of the corn seeds in order to ensure that the seeds can enter the seed cavity smoothly. Demeiya No. 1 was used as the test seed, and 100 seeds were chosen to measure its triaxial size of 10.06 mm, 8.13 mm, and 5.21 mm. As a result, the pick's length and width were calculated to be 11 mm and 11 mm, respectively. The geometric size parameters of the pick are shown in Figure 5, and the thickness of the pick is determined to be c = 1 mm in order to ensure its strength.

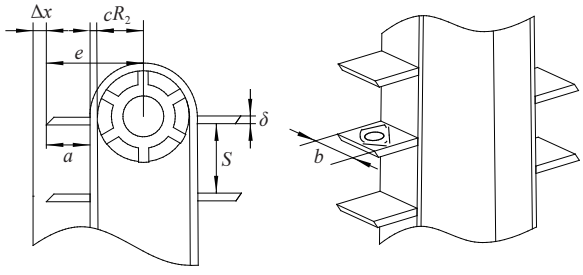

a. Side view b. Isometric view

Figure 5 Structure and size chart of the pick

2.2.6 Calculation of pick spacing and number of seed cavities

On the seed conveying belt's surface, the picks are dispersed uniformly. The distance between the picks determines the size of the seed cavity when the length of the seed conveying belt is fixed. The following is the calculation equation:

$$Z = \frac{L}{S} \tag{3}$$

where, Z is the number of picks on the seed conveying belt; L is the length of the seed conveying belt, mm; S is the distance between adjacent picks, mm.

The pick on the seed conveying belt rotates N times as many

times as the seeds on the seed disk within time t, and their relationship can be expressed as Equation (4):

$$Nn_1Kt = \frac{V_2 t}{S} \tag{4}$$

where, n_1 is the rotating speed of the seed disk, r/m; K is the number of holes in the seed disk; V_2 is the speed of seed throwing.

The rotation speed of the seed disk is calculated by Equation (5):

$$n_1 = \frac{V_0}{KD} \tag{5}$$

where, V_0 is the advance speed of sowing, m/s; D is the distance between adjacent seeds in the seed ditch, m.

The rotating speed of the driving pulley is calculated by Equation (6):

$$V_2 = \pi n_2 (R_2 + e) \tag{6}$$

where, n_2 is the rotational speed of the driving pulley, r/s; R_2 is the radius of the driving pulley, mm; e is the baseband thickness of the seed conveying belt, mm.

Substituting Equation (6) into Equation (4):

$$Nn_1K = \frac{2\pi n_2 (R_2 + e)}{S} \tag{7}$$

The pick on the seed conveying belt rotates N times as frequently within time t as seeds are thrown into the seed ditch at the same time.

$$\frac{NV_0 t}{D} = \frac{V_2 t}{S} \tag{8}$$

Equation (4) and Equation (8) are combined to obtain:

$$V_0 = Kn_1 D \tag{9}$$

From Equation (7):

$$S = \frac{2\pi (R_2 + e) i_{21}}{NK} \tag{10}$$

Among them:

$$i_{21} = \frac{n_2}{n_1} \tag{11}$$

where, i_{12} is the ratio of the rotational speed of the driving pulley to the disk.

The size of the corn seeds should be taken into consideration when choosing the pick spacing. Small pick spacing can increase the effectiveness of the seed conveying belt in guiding the seed, but it can also cause larger seeds to miss sowing because they cannot fit into the seed cavity. Even though it is advantageous for the seeds to enter the seed cavity, if the pick spacing is large, the seed cavity's ability to restrain the seeds will suffer, which will reduce the stability of the seeds in the seed cavity.

The integer multiple N = 5 is established, which means that adjacent seeds are separated by 4 seed cavities, taking into account the seed guiding effectiveness and the speed of the seed conveying belt. The seed conveying belt that complies with the requirements can have pick spacings of 10, 15, or 20 mm, and has 118, 79, or 59 seed cavities. Accordingly, the speed ratio between the driving pulley and the seed disk is 13.45, 20.08, or 26.89. In this study, in order to select the appropriate number of seed cavities, it was determined by discrete element simulation[17-21].

2.3 Theoretical analysis of seed transportation process

2.3.1 Mechanical analysis of seeds in receiving

Ectopic seeds will result from the seeds colliding with the pick during the seed receiving stage. Figure 6 displays the force analysis of the seeds.

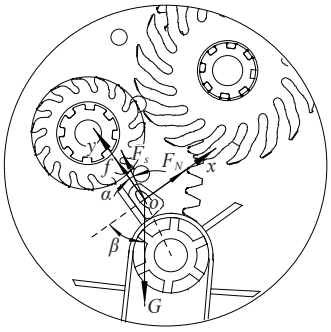

Figure 6 Stress on seeds during receiving

The direction perpendicular to the pick serves as the abscissa and the direction parallel to the pick serves as the ordinate in a coordinate system. The force acting on the seed in the positive direction of the y axis should be less than or equal to the force acting on the seed in the negative direction of the y axis in order to minimize collisions between the seed and the pick. Equation (12) illustrates the seed's force equation:

$$\begin{cases} F_s\cos\alpha + f \le G\sin\beta \\ F_s = m\omega^2 (R_2 + e) \\ f = \mu F_{\mathrm{N}} \\ F_{\mathrm{N}} = G\cos\beta \\ G = mg \end{cases} \tag{12}$$

where, F_S is the centrifugal force of the seed conveying belt on the seeds, N; F_N is the support of the pick to the seed, N; f is the friction of the pick on the seed, N; G is the gravity of the seeds, N; m is the mass of the seeds, kg; ω is the rotational angular velocity of the seed conveying belt, rad/s; α is the angle between the centrifugal force and Y-axis, (°); β is the angle between gravity and the X-axis, (°); μ is the friction coefficient between the pick and seed.

Based on the above equation, we can get:

$$\omega \le \sqrt{\frac{g(\sin\beta - \mu\cos\beta)}{(R_2 + e)\cos\alpha}} \tag{13}$$

In reality, the adjustment ranges for the included angles of gravity and the X-axis are 10°–75°, and for the centrifugal force and the Y-axis are 0°–10°, and the friction coefficient between the seed and the pick is constant. The critical rotation speed of the seed leaving the seed cavity, calculated from the data, is 28.11 r/s. When the pick spacing is 10 mm, the pulley speed is 14.69 r/s; when the pick spacing is 15 mm, the pulley speed is 18.36 r/s; and when the pick spacing is 20 mm, the pulley speed is 22.03 r/s. These pulley speeds are all less than the critical value, ensuring that there is only a minor collision between the seeds and the pick.

2.3.2 Mechanical analysis of seeds in throwing

The time required for two adjacent picks to rotate to the same position is:

$$t_0 = \frac{S}{V_2} \tag{14}$$

At the same time, the displacement of the dropped seed is shown in the following Equation (15):

$$H = V_2 t\sin\gamma + \frac{1}{2} g t_0^2 \tag{15}$$

where, H is the displacement of the dropped seed, mm; γ is the angle of seed throwing, (°); t_0 is the time of the seed falling from the seed throwing position to the seed ditch, s.

Summing up Equations (3)-(6), (14), and (15), Equation (16)

can be obtained.

$$H = S\sin\gamma + \frac{S^2 g}{8\pi^2 n_2^2 (R_2 + e)} \tag{16}$$

When the spacing is 10 mm, the falling displacement of the seeds is 11.59 mm; when the pick spacing is 15 mm, the falling displacement of the seeds is 14.49 mm; and when the spacing of the paddles is 20 mm, the falling displacement of the seeds is 17.39 mm. The range of values for the angle of seed throwing is 65°–85°. The pick will not obstruct seed delivery when the maximum size of seeds is 10 mm because the falling displacement of the seeds is greater than the size of the seeds at any given time.

2.3.3 Analysis of seed throwing trajectory

The seed throwing speed and trajectory at the throwing position are shown in Figure 7.

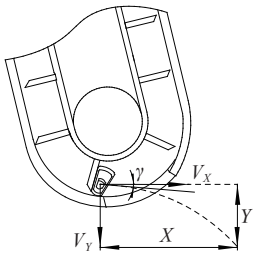

Figure 7 Schematic diagram of seeding speed and trajectory

In order to prevent the seeds from colliding with the soil, the horizontal speed of the seeds should cancel out with the forward speed of sowing. And the trajectory equation can be obtained:

$$\begin{cases} x = V_x t \\ y = V_y t + \dfrac{1}{2} g t^2 \\ V_x = V_2\cos\gamma - V \\ V_y = V_2\sin\gamma \end{cases} \tag{17}$$

where, x is the horizontal displacement of the seeds; γ is the vertical displacement of the seeds, that is, the height of the seed guide device from the ground; V_x is the speed of seeds in the horizontal direction; V_y is the speed of seeds in the vertical direction.

Based on the above Equation (17), we can get Equation (18):

$$x = \frac{V_2\cos\gamma - V}{g}\left[\sqrt{2gY - V_2^2\sin^2\gamma} - \left(V_2\cos\gamma - V\right)\right] \tag{18}$$

The mathematical model described above indicates that the horizontal displacement of the seed is primarily influenced by the seed's initial speed, forward speed, height above the ground, and throwing angle. The rotational speed of the seed conveying belt, which is directly correlated to the spacing between adjacent seeds measured in the seed cavities, determines the seed throwing speed. Therefore, in the seed throwing process, the number of seed cavities between adjacent seeds, the advancing speed, the height of the seed guide device from the ground, and the installation angle of the seed guide device all have a significant impact on the seed movement trajectory.

2.4 Simulation analysis of seed guiding process based on EDEM

2.4.1 Establishment of simulation model

The three-dimensional drawing software NX 12.0 is used to model the seed guide device, and it is saved in IGS format and imported into EDEM software[22,23]. The model diagram of different pick spacings is shown in Figure 8.

The seed conveying belt of the seed guiding device is made of polyurethane, and the rear shell and the two side shells are made of high-pressure polyethylene resin[24-27]. In order to observe the seed guiding situation conveniently, the front shell is made of plexiglass, and the material parameters are listed in Table 1.

In the previous design, the average triaxial size of the seeds was 10.06 mm×8.13 mm×5.21 mm. The corn seed model was established in UG software, and the model was saved in STEP format and imported into EDEM software. The model was constructed with 10 filled spheres. The filling diagram is shown in Figure 9, and the Poisson's ratio of the seeds was set to 0.4, the shear modulus was 1.37×10^8 Pa, and the density was 197 kg/m^3[28-30].

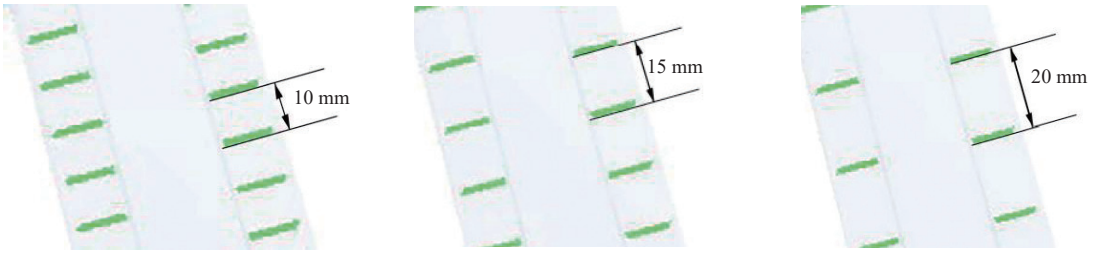

a. 10 mm b. 15 mm c. 20 mm

Figure 8 Simulation model diagram of different pick spacings

Table 1 Material parameters

Material	Polyurethane	High-pressure polyethylene resin	Plexiglass
Poisson's ratio	0.42	0.35	0.5
Shear modulus/Pa	3.768×10^7	2.45×10^8	1.77×10^8
Density/g·cm^{-1}	1.65	1.6	1.18

2.4.2 Simulation results and analysis

Taking the number of seed cavity intervals as the simulation test factor, each group of experiments was repeated three times, and the average value was calculated. The qualified rate, rebroadcast rate, missed seeding rate, and variation coefficient are selected as

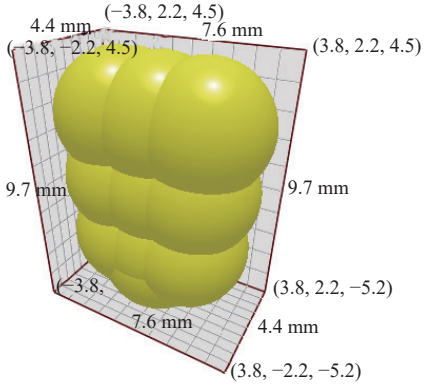

Figure 9 Seed particle filling diagram

virtual test indexes[31-33]. In order to observe the changing trend of the performance of the seed guide device with the test factors more intuitively, the corresponding index trend curve is drawn, as shown in Figure 10.

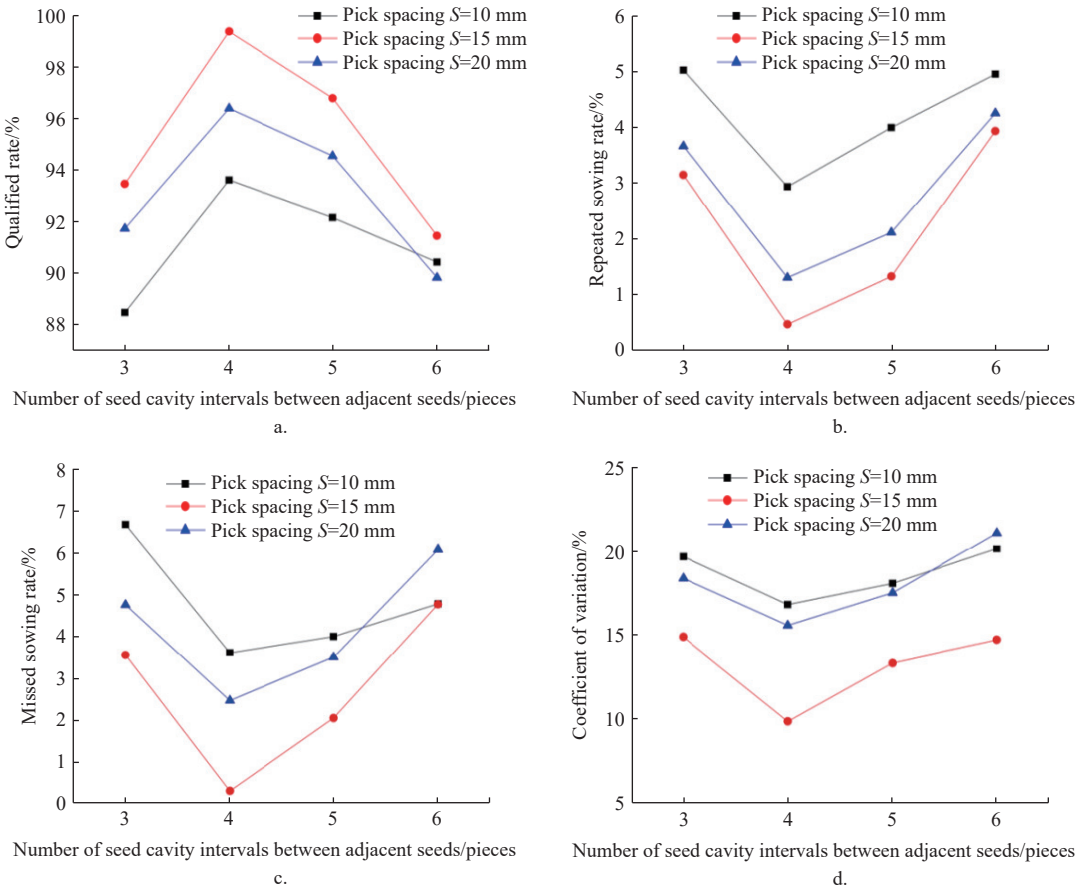

Figure 10 Curve of simulation test results

As can be seen from Figure 10, when the pick spacing is 15 mm, the qualified rate is the highest, and the repeated-missed sowing rate and the coefficient of variation are the lowest. At the same time, when the number of corresponding seed cavity intervals is 4, the qualified rate, repeated-missed sowing rate, and coefficient of variation of seed spacing reach their best states. Therefore, the spacing between picks is 15 mm, and the number of seed cavities is 79. The pick spacing is set to 15 mm, and then the simulation test is repeated three times to verify the results. The average values of the simulation test results are 99.34% qualified rate, 0.42% repeated sowing rate, 0.24% missed sowing rate, and 8.97% coefficient of variation. The test results show that the parameters are accurate and reliable.

2.5 Bench test

The corn seed variety chosen for the test was Demeiya No. 1, and the testing location was Heilongjiang Bayi Agricultural University's sowing lab. As shown in Figure 11, the test bench was a JPS-16 high-speed sowing performance test bench.

An orthogonal rotation combination experiment with three factors and five levels was conducted under the assumption of a sowing speed of 16 km/h. The number of seed cavity intervals between adjacent seeds, the height from the ground, and the seed guide device's inclination angle are the main variables affecting the performance of the device, according to the previous theoretical analysis. As a result, these three factors are chosen as the test factors, and the factor coding table is listed in Table 2. The coefficient of variation, repeated sowing rate, missed sowing rate, and qualified rate were chosen as the test indices.

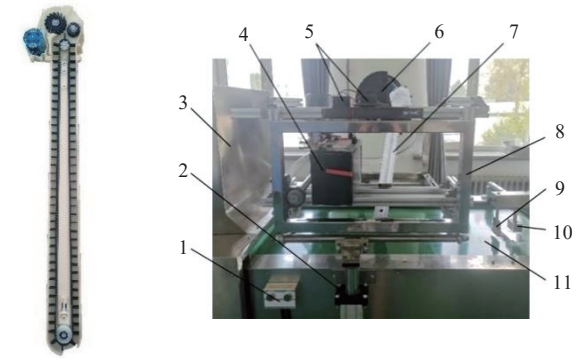

a. Guide device b. Test bench

1. Device height above ground controller. 2. Hydraulic cylinder. 3. Seed image capture device. 4. Storage battery. 5. Speed controller. 6. Seed-metering device. 7. Belt-type high-speed corn seed guiding device. 8. Carriage. 9. Oil brush. 10. Oil-out port. 11. Conveyor belt.

Figure 11 JPS-16 high-speed seeding performance test bench and guide device

Table 2 Coding table of test factors

Coded value	Number of seed cavity intervals between adjacent seeds/individual	Installation angle/(°)	Height from the ground/mm
+1.682	7	84	40
+1	6	82	36
0	5	80	30
−1	4	78	24
−1.682	3	76	20

3 Results and discussion

3.1 Result analysis

Each group of experiments was repeated three times, and the average value was taken as the test result, as listed in Table 3. The variance analysis table is presented in Table 4 and was created using the data processing software Design-Expert.

Table 3 Test results

Order-number	Factor			Index			
	Number of seed cavity intervals between adjacent seeds/ individual	Installation angle/ (°)	Height from the ground/ mm	Qualified rate/%	Repeated sowing rate/%	Missed sowing rate/%	Coefficient of variation/ %
1	1	1	1	92.32	1.11	6.57	14.21
2	1	1	–1	94.03	2.25	3.72	12.05
3	1	–1	1	92.52	0.74	6.74	13.48
4	1	–1	–1	90.92	1.92	7.16	17.45
5	–1	1	1	93.27	0.91	5.82	13.63
6	–1	1	–1	95.53	1.45	3.02	7.46
7	–1	–1	1	91.21	1.08	7.71	15.28
8	–1	–1	–1	93.38	0.87	5.75	13.46
9	1.682	0	0	90.23	0.92	8.85	16.54
10	–1.682	0	0	92.03	2.76	5.21	13.03
11	0	1.682	0	92.82	0.97	6.21	9.68
12	0	–1.682	0	90.26	0.87	8.87	16.84
13	0	0	1.682	92.16	1.46	6.38	9.98
14	0	0	–1.682	95.64	0.31	4.05	10.59
15	0	0	0	97.91	0.37	1.72	8.65
16	0	0	0	98.72	0.32	0.96	7.02
17	0	0	0	97.32	0.71	1.97	8.11
18	0	0	0	98.48	0.38	1.14	7.39
19	0	0	0	98.33	0.59	1.08	6.71
20	0	0	0	99.28	0.23	0.49	6.34
21	0	0	0	96.35	0.31	3.34	8.28
22	0	0	0	99.61	0.28	0.11	5.74
23	0	0	0	98.54	0.64	0.82	7.31

3.1.1 Establishment of qualified rate and regression model of various factors

The quadratic regression model of the qualified rate $p<0.01$ is listed in Table 3 and is seen to be extremely significant under the assumption of a significance level of 0.05. The determining coefficient of the regression equation is shown to be 0.9503, which demonstrates that the predicted value of the regression equation has a high degree of fitting with the actual value of the test. Following the elimination of irrelevant variables, the regression equation is as follows:

$$Y_1 = -1.82X_1^2 - 1.72X_2^2 - 1.66X_3^2 + 0.51X_1 - 0.77X_2 + 0.69X_3 + 98.26 \quad (19)$$

3.1.2 Establishment of repeated rate and regression model of various factors

According to Table 3, under the condition of the significance level of 0.05, the quadratic regression model of the repeated sowing rate $p<0.01$ is extremely significant. The determining coefficient of the regression equation is shown to be 0.9503, which demonstrates that the predicted value of the regression equation has a high degree of fitting with the actual value of the test. Following the elimination of irrelevant variables, the regression equation is as follows:

Table 4 Analysis of variance

Evaluating indicator	Source of variance	Sum of squares	Freedom	Mean square	F-value	P-value	Significance
Qualified rate Y_1	Model	211.47	9	23.50	27.64	<0.0001	**
	X_1	4.14	1	4.14	4.87	0.0459	*
	X_2	9.36	1	9.36	11.01	0.0055	**
	X_3	6.52	1	6.52	7.67	0.0159	**
	X_1X_2	1.44	1	1.44	1.70	0.2149	–
	X_1X_3	2.33	1	2.33	2.74	0.1215	–
	X_2X_3	0.2112	1	0.2112	0.2485	0.6265	–
	X_{12}	94.37	1	94.37	111.01	<0.0001	**
	X_{22}	84.06	1	84.06	98.88	<0.0001	**
	X_{32}	41.87	1	41.87	49.26	<0.0001	**
	Residual	11.05	13	0.8501	–	–	–
	Lack of Fit	3.20	5	0.6390	0.6508	0.6698	–
	Pure Error	7.86	8	0.9820	–	–	–
	Cor Total	222.52	22	–	–	–	–
Repeated sowing rate Y_2	Model	8.95	9	0.9944	18.70	<0.0001	**
	X_1	2.50	1	2.50	47.11	<0.0001	**
	X_2	0.1073	1	0.1073	2.02	0.1790	–
	X_3	0.9703	1	0.9703	18.25	0.0009	**
	X_1X_2	0.0630	1	0.0630	1.19	0.2961	–
	X_1X_3	0.4950	1	0.4950	9.31	0.0093	**
	X_2X_3	0.0105	1	0.0105	0.1977	0.6639	–
	X_{12}	4.04	1	4.04	76.08	<0.0001	**
	X_{22}	0.6180	1	0.6180	11.62	0.0047	**
	X_{32}	0.7217	1	0.7217	13.57	0.0028	**
	Residual	0.6911	13	0.0532	–	–	–
	Lack of Fit	0.4481	5	0.0896	2.95	0.0843	–
	Pure Error	0.2430	8	0.0304	–	–	–
	Cor Total	9.64	22	–	–	–	–
Missed sowing rate Y_3	Model	167.09	9	18.57	25.96	<0.0001	**
	X_1	13.09	1	13.09	18.30	0.0009	**
	X_2	11.48	1	11.48	16.05	0.0015	**
	X_3	2.46	1	2.46	3.44	0.0865	–
	X_1X_2	2.11	1	2.11	2.95	0.1094	–
	X_1X_3	0.6786	1	0.6786	0.9490	0.3478	–
	X_2X_3	0.1275	1	0.1275	0.1783	0.6797	–
	X_{12}	59.34	1	59.34	82.98	<0.0001	**
	X_{22}	70.26	1	70.26	98.25	<0.0001	**
	X_{32}	31.60	1	31.60	44.19	<0.0001	**
	Residual	9.30	13	0.7151	–	–	–
	Lack of Fit	2.02	5	0.4036	0.4436	0.8071	–
	Pure Error	7.28	8	0.9098	–	–	–
	Cor Total	176.39	22	–	–	–	–
Coefficient of variation Y_4	Model	283.25	9	31.47	18.16	<0.0001	**
	X_1	10.89	1	10.89	6.28	0.0262	*
	X_2	44.36	1	44.36	25.60	0.0002	**
	X_3	2.97	1	2.97	1.71	0.2133	–
	X_1X_2	13.73	1	13.73	7.92	0.0146	*
	X_1X_3	12.00	1	12.00	6.93	0.0207	*
	X_2X_3	1.11	1	1.11	0.6406	0.4379	–
	X_{12}	119.46	1	119.46	68.94	<0.0001	**
	X_{22}	79.20	1	79.20	45.71	<0.0001	**
	X_{32}	32.72	1	32.72	18.88	0.0008	**
	Residual	22.53	13	1.73	–	–	–
	Lack of Fit	15.30	5	3.06	3.39	0.0614	–
	Pure Error	7.23	8	0.9033	–	–	–
	Cor Total	305.78	22	–	–	–	–

$$Y_2 = 0.38xX_1^2 + 0.15X_2^2 + 0.22X_3^2 - 0.25X_1X_3 + 0.40X_1 - 0.27X_3 + 0.44 \quad (20)$$

3.1.3 Establishment of missed sowing rate and regression model of various factors

The regression equation's determination coefficient between the missed sowing rate and various factors is 0.9473, indicating that the predicted value of the regression equation fits the test result very closely. Following the elimination of irrelevant variables, the regression equation is as follows:

$$Y_3 = 1.45X_1^2 + 1.57X_2^2 + 1.44X_3^2 - 0.90X_1 + 0.85X_2 - 0.27X_3 + 1.30 \quad (21)$$

3.1.4 Establishment of coefficient of variation and regression model of various factors

The regression equation's determination coefficient between the coefficient of variation and various factors is 0.9263, indicating that the predicted value of the equation fits the test result very closely. Following the elimination of irrelevant variables, the regression equation is as follows:

$$Y_4 = 2.05X_1^2 + 1.67X_2^2 + 1.46X_3^2 + 1.31X_1X_2 - 1.22X_1X_3 - 0.83X_1 + 1.66X_2 + 7.38 \quad (22)$$

3.2 Optimization and verification of results

The test data are optimized to obtain the ideal parameter combination for each test factor, and the following mathematical model for parameter optimization is developed:

$$\begin{cases} \max Y_1 \\ \min Y_2 \\ \min Y_3 \\ \min Y_4 \\ 3 \le X_1 \le 7 \\ 76^\circ \le X_2 \le 84^\circ \\ 20\ \text{mm} \le \text{X}_3 \le 40\ \text{mm} \\ 0\% \le Y_1(X_1, X_2, X_3) \le 100\% \\ 0\% \le Y_2(X_1, X_2, \text{X}_3) \le 100\% \\ 0\% \le Y_3(X_1, X_2, X_3) \le 100\% \\ 0\% \le Y_4(X_1, X_2, X_3) \le 100\% \end{cases} \quad (23)$$

The mathematical model is optimized using Design-Expert 12's optimization module[34-36]. The best seed guiding device performance parameters are: a qualified rate of 98.49%, repeated sowing rate of 0.48%, missed sowing rate of 1.03%, and coefficient of variation of 1.03% when the number of seed cavity intervals between adjacent seeds is 5.16, the installation angle is 79.40, and the height from the ground is 31.84 mm.

The verification test was executed based on the optimization results. According to the experimental findings, the qualified rate is 98.62%, the rate of repeated sowing is 0.42%, the rate of missed sowing is 0.96%, and the coefficient of variation is 7.02%. This satisfies the criteria for precision and quick corn sowing while having a small error in the optimized data[37-39].

4 Conclusions

(1) A belt-type high-speed corn seed guiding device's seed receiving and conveying system was designed and optimized. The seed-receiving gap width, the minimum deformation value and the maximum deformation value, finger structure and parameters, pick size parameters, and the number of seed cavities were confirmed. Force analysis was performed in the seed receiving and throwing stages. The influencing factors of horizontal displacement were obtained. They were the seed's initial speed, forward speed, height above the ground, and the seed's throwing angle. The critical rotation speed was obtained also, and the pulley speeds are all less than the critical value.

(2) The qualification rate was the highest, the missed seeding rate was the lowest, and the coefficient of variation was the lowest when the picking spacing and the number of corresponding seed cavity intervals were 15 mm and 4 when using the DEM simulation software. Then the three factors and five-level quadratic orthogonal rotation combination tests and variance analysis were operated. The regression models were established between each test factor and evaluation index.

(3) The optimizing experiments showed that when the seed cavity intervals between adjacent seeds were 5, the installation angle was 79°, and the height from the ground was 32 mm, the performance of the seed introduction was the best. According to the experimental findings, the qualified rate was 98.62%, the rate of repeated sowing was 0.42%, the rate of missed sowing was 0.96%, and the coefficient of variation was 7.02%.

Acknowledgements

This research was financially supported by the National Natural Science Foundation (Grant No. 52275246), and the Key Research and Development Plan Project of Heilongjiang Province (Grant No. 2022ZX05B02).

[References]

[1] Li Y H, Yang L, Zhang D X, Cui T, He X T, Du Z H, et al. Performance analysis and structure optimization of the maize precision metering device with air suction at high-speed condition. Transactions of the CSAE, 2022; 38(8): 1–11. (in Chinese)

[2] Yang W. Research on key technologies and equipment for precision sowing of maize breeding. PhD thesis, Chinese Academy of Agricultural Mechanization Sciences, Beijing, China, 2019. (in Chinese)

[3] Yang L, Yan B X, Cui T, Yu Y M, He X T, Liu Q W. Global overview of research progress and development of precision maize planters. Int J Agric & Biol Eng, 2016; 9(1): 9–26.

[4] Yuan Y W, Bai H J, Fang X F, Wang D C, Zhou L M, Niu K. Research progress on maize seeding and its measurement and control technology. Transactions of the CSAM, 2018; 49(9): 1–18. (in Chinese)

[5] Yang L, Yan B X, Zhang D X, Zhang T L, Wang Y X, Cui T. Research progress on precision planting technology of maize. Transactions of the CSAM, 2016; 47(11): 38–48. (in Chinese)

[6] Hou L Y, Zhang X F, Feng G, Li Z, Zhang Y B, Cao N. Arbuscular mycorrhizal enhancement of phosphorus uptake and yields of maize under high planting density in the black soil region of China. Scientific Reports, 2021; 11(1): 1–11. (in Chinese)

[7] Tang H, Xu C S, Wang Z M, Wang Q, Wang J W. Optimized design, monitoring system development and experiment for a long-belt finger-clip precision corn seed metering device. Frontiers in Plant Science, 2022; 13: 814747.

[8] Zhang B F, Liu D, Xi X B, Zhang Y F, Chen C, Qu J W, et al. The analysis of the applications of crop seed tape sowing technology and equipment: A review. Applied Sciences, 2021; 11(23): 11228.

[9] Searle C L, Kocher M F, Smith J A, Blankenship E E. Field slope effects on uniformity of corn seed spacing for three precision planter metering systems. Applied Engineering in Agriculture, 2008; 24(5): 581–586.

[10] Zhou B D, Li Y X, Zhang C, Cao L W, Li C S, Xie S J. Potato planter and planting technology: A review of recent developments. Agriculture, 2022; 12(10): 1600.

[11] Kovács P, Casteel S N. Evaluation of a high‐speed planter in soybean production. Agronomy Journal, 2023; 115(3): 1174–1187.

[12] John Deere. ExactEmerge high-speed planter. https://www.deere.com/en/

planting-and-seeding-equipment/planters/exactemerge-high-speed-planter/.
[13] Wei M J, Diao P S, Wang W J. Design and experiment of the seed delivery device with a rotating brush wheel for precision seeder. Engenharia Agrícola, 2022; 42(6): e20220089.
[14] Nielsen R L. Stand establishment variability in corn. Proceedings of the Integrated Crop Management Conference. Iowa State University, Digital Press, 1993.
[15] Zhu H B, Wu X, Bai L Z, Li R N, Guo G, Jin Q, et al. Design and experiment of a soybean shaftless spiral seed discharge and seed delivery device. Scientific Reports, 2023; 13(1): 20751.
[16] Chen X G, Zhong L M. Design and test on belt-type seed delivery of air-suction metering device. Transactions of the CSAE, 2012; 28(22): 8–15.
[17] Liu R. , Liu L J, Li Y J, Liu Z J, Zhao J W, Liu Y Q, et al. Numerical simulation of seed-movement characteristics in new maize delivery device. Agriculture, 2022; 12(11): 1944.
[18] Ma C C, Yi S J, Tao G X, Li Y F, Wang S, Wang G Y, et al. Research on receiving seeds performance of belt-type high-speed corn seed guiding device based on discrete element method. Agriculture, 2023; 13(5): 1085.
[19] Jia H L, Chen Y L, Zhao J L, Guo M Z, Huang D Y, Zhuang J. Design and key parameter optimization of an agitated soybean seed metering device with horizontal seed filling. Int J Agric & Biol Eng, 2018; 11(2): 76–87.
[20] Liu Q W, Cui T, Zhang D X, Yang L, Wang Y X, He X T, et al. Design and experimental study of seed precise delivery mechanism for high-speed maize planter. Int J Agric & Biol Eng, 2018; 11(4): 81–87.
[21] Zhao X S, Bai W J, Li J C, Yu H L, Zhao D W, Yin B Z. Study on positive-negative pressure seed metering device for wide-seedling-strip-seeding. Int J Agric & Biol Eng, 2022; 15(6): 124–133.
[22] Ding Y Q, Yang L, Zhang D, Cui T, Li Y H, Zhong X P, et al. Novel low-cost control system for large high-speed corn precision planters. Int J Agric & Biol Eng, 2021; 14(2): 151–158.
[23] Liu W, Zou S S, Xu X L, Gu Q Y, He W Z, Huang J, et al. Development of UAV-based shot seeding device for rice planting. Int J Agric & Biol Eng, 2022; 15(6): 1–7.
[24] Zhang W X, Wang F Y. Parameter calibration of American ginseng seeds for discrete element simulation. Int J Agric & Biol Eng, 2022; 15(6): 16–22.
[25] Esterhuizen M, Kim Y J. Effects of polypropylene, polyvinyl chloride, polyethylene terephthalate, polyurethane, high-density polyethylene, and polystyrene microplastic on Nelumbo nucifera (Lotus) in water and sediment. Environ Sci Pollut Res, 2022; 29(6): 17580–17590.
[26] Gu F W, Zhao Y Q, Feng W, Hu Z C, Shi L L. Simulation analysis and experimental validation of conveying device in uniform rushed straw throwing and seed-sowing machines using CFD-DEM coupled approach. Computers and Electronics in Agriculture, 2022; 193: 106720.
[27] Lu J Q, Yang Y, Li Z H, Shang Q Q, Li J C, Liu Z Y. Design and experiment of an air-suction potato seed metering device. Int J Agric & Biol Eng, 2016; 9(5): 33–42.
[28] Yazgi A, Degirmencioglu A. Measurement of seed spacing uniformity performance of a precision metering unit as function of the number of holes on vacuum plate. Measurement, 2014; 56: 128–135.
[29] Liu Z Y, Xia J F, Hu M J, Du J, Luo C M, Zheng K. Design and analysis of a performance monitoring system for a seed metering device based on pulse width recognition. PloS One, 2021; 16(12): e0261593.
[30] Önal S, Degirmencioglu A, Yazgi A. An evaluation of seed spacing accuracy of a vacuum type precision metering unit based on theoretical considerations and experiments. Turkish Journal of Agriculture and Forestry, 2012; 36(2): 133–144.
[31] Lei X L, Hu H J, Yang W H, Liu L Y, Liao Q, Wang R. Seeding performance of air-assisted centralized seed-metering device for rapeseed. Int J Agric & Biol Eng, 2021; 14(5): 79–87.
[32] Wang B L, Na Y, Liu J, Wang Z M. Design and evaluation of vacuum central drum seed metering device. Applied Sciences, 2022; 12(4); 2159.
[33] Guo J, Yang Y, Memon M S, Tan C, Wang L Y, Tang P. Design and simulation for seeding performance of high-speed inclined corn metering device based on discrete element method (DEM). Scientific Reports, 2022; 12(1): 19415.
[34] Sopyan I, Gozali D, Kurniawansyah I S, Guntina R K. Design-expert software (DOE): An application tool for optimization in pharmaceutical preparations formulation. International Journal of Applied Pharmaceutics, 2022; 14(4): 55–63.
[35] Hossain M S, Jahan S, Rahman S A R, Rahman M, Shill D K, Paul S, et al. Design expert software assisted development and evaluation of empagliflozin and sitagliptin combination tablet with improved in-vivo anti-diabetic activities. Heliyon, 2023; 9(3): e14259.
[36] Arpna I, Masheer K A. Box-Behnken design for optimization of formulation variables for controlled release gastroretentive tablet of verapamil hydrochlorid. International Journal of Applied Pharmaceutics, 2023; 15(1): 256–263.
[37] Djaman K, Allen S, Djaman D S, Koudahe K, Irmak S, Puppala N, et al. Planting date and plant density effects on maize growth, yield and water use efficiency. Environmental Challenges, 2022; 6: 100417.
[38] Zhang Y H, Xu Z G, Li J, Wang R. Optimum planting density improves resource use efficiency and yield stability of rainfed maize in semiarid climate. Frontiers in Plant Science, 2021; 12: 752606.
[39] Clemente O G, Albajes R, Batuecas I, Achon M A. Planting period is the main factor for controlling maize rough dwarf disease. Scientific Reports, 2021; 11(1): 977.